Astronomy & Astrophysics (Caucasus) 5, (2020)

CATALOG KVARATSKHELIA-SAARI-SHORTHILL

O. I. KVARATSKHELIA

E. Kharadze National Astrophysical Observatory

Email: kvara_otar@mail.ru

Abstract
The studies accomplished at the end of the past century, comparing various optical characteristics of lunar soils and their terrestrial analogs, showed that it is possible to identify different degrees of packing of the lunar surface matter by remote sensing methods. The normal albedo ρ0 and the maximum degree of polarization Pm are used as the initial characteristics of the reflectivity of a finely dispersed substance.
Key words: Moon, Polarization, Albedo

It was found that on a two-dimensional histogram of the ρ0 (Pm) type, among the points of measured albedo values and the maximum degree of polarization of a number of finely dispersed terrestrial magmatic samples of a known grain-size and mineralogical composition, two types of sequences can be distinguished. One family of functions characterizes changes in ρ0 and Pm of a substance of the same type with insignificant variation in chemical composition. Another is a change in the optical characteristics of rocks with similar particle diameters, with a change in the mineralogical and chemical composition [1]. Test studies were carried out in the area of volcanic deposits in Kamchatka, based on polarized aerial photography [2].

The results of numerous studies of analogs of lunar soil made it possible to introduce the concept of an optical parameter of the relative porosity of a reflecting substance of the following form: $\Delta\Psi = il g\rho + klgP$m, which quantitatively describes the ability of the uppermost soil layer to absorb and scatter sunlight [3].

This parameter (in a simplified form ρ0 (Pm)) is physically close to the second non-normalized Stokes parameter. An analysis of the cumulative results showed that the adopted parameter shows the real relationship between the physical and the mechanical properties of the soil in its natural bedding with the characteristics of scattered light and describes the properties of not only a reflecting optically thin layer of matter, but also deeper underlying layers. The technique makes it possible to identify large-scale irregularities in the density of the material using synthesized images.

A number of studies in this direction make it clear that it is possible to assess the effective size of particles of a finely dispersed material in the surface layer [4]. As a result of laboratory measurements, the ratio between the normal albedo, the maximum degree of polarization and the average particle size was obtained: lgΔΨ=4,8lgρ0+ 3,4lgpm-7,1.

Identification of areas with a predominant distribution of the fine fraction in the surface layer of the Moon is extremely important at the early stages of design work on the lunar base, since it is in the mass of the fine fraction that the largest amount of hydrogen and helium-3, the main elements of the natural resources of the Moon, is contained. As it is known from the works by various authors, over 80% of hydrogen and helium-3 in the samples of lunar rocks delivered to the Earth was found in a fine fraction with a particle size of up to 45 microns. From this point of view, according to our data [1], the south of the Sea of Abundance is promising.

One of the most important practical conclusions made by B. Hapke [5] in the theoretical consideration of the phase function of the Moon was the determination of the parameter of the relative density of lunar surface H. This value characterizes the packing of particles of the uppermost extremely fragmented and

porous layer of the lunar regolith. The Hapke values of this parameter are determined by the following formula $H=K\sqrt[3]{(d/d_0)^2}$ .Here d0 is the density of the rock, d is the density of the lunar surface rocks, the coefficient K = 2 for the lunar sites. Measurements of parameter H over the lunar disk for small areas (~10") revealed significant differences in H from place to place within 0.1 <H <1.1 [6], with an average value of the relative density parameter for the visible hemisphere of the Moon equal to 0.5. Mapping of this parameter directly using the formulas of the Hapke photometric function is possible only by points. At the same time, it would be very useful to know the prevalence of this parameter over the lunar disk to reveal the presence of large-scale non-homogeneities in the relative density of the lunar surface.
We set the task to reveal the relationship between the Hapke parameter - H and the optical parameter of relative porosity. For this purpose, on the 40-cm Zeiss refractor of the Abastumani Astrophysical Observatory (F = 6.8m) at a wavelength ƛ = 0.440 μm, with a working aperture d = 7 ". 5, at close phases for both quarters of the moon, in quadratures, when the degree polarization reaches its maximum value (phase angle α~ ±900), O. Kvaratskhelia accomplished polarimetric observations of all points of the Saari-Shorthill catalog [6], for which the normal albedo was measured with high accuracy.
The observations were accomplished using an automatic electro-polarimeter of the Abastumani Astrophysical Observatory [7]. The results of these observations for 190 points of the catalog [6] (77 points for the first quarter and 113 for the last one) were published in article [8] as KVARATSKHELIA-SAARI-SHORTHILL catalog. Additional polarimetric observations of objects from the Saari-Shorthill catalog with the same equipment were accomplished in 2005-2009 [9, 10, 11].

This article presents the results for about 300 catalog points [7]. At the end of the article, we present the complete KVARATSKHELIA-SAARI-SHORTKHILL catalog with the following designations: ƛ, β-selenographic coordinates of the observed areas; HX100 is the Hapke parameter and ρ0% is the normal albedo of the sites according to the catalog [6]; Pm% is the results of polarimetric observations by O. Kvaratskhelia; ρ0 (Pm)is the parameter corresponding to the second unnormalized Stokes parameter in a physical sense and being proportional to ΔΨ; the index is the qualitative characteristics of the lunar regions according to the catalog [6]. For example: A designates area with medium albedo, B means bright, D means dark, C is the craters, etc. α is the angle of the moon phase during the observations. At the end of the work, Moon maps are given, which are taken from the Saari-Shorthill catalog [6] with the designations of the measured lunar areas, Fig. 4a - 12a, for the western hemisphere of the Moon and Fig. 4b - 12b, for the eastern hemisphere of the moon.
The observation results are as follows:
1. Based on our subsequent observations to the photo-polarimetric catalog of Kvaratskhelia-Saari-Shorthill [8], the polarization data have been added. Now, the catalog for 284 lunar surface objects consists of the following data: normal albedo, Hapke parameter and degree of polarization.
2. We compared the values of the Hapke parameter and the product ρ0 (Pm) at each observation point [8], and did not reveal a direct relationship between them. Then we compared the average values of ρ0 (Pm), at the intervals of changes in the parameter H: 0.1-0.2, 0.2-0.3, etc. [8]. In this case, a clear direct dependence of changes in ρ0 (Pm) and the Hapke parameter was revealed, and it is individual for each quarter. This result needs to be verified, since it is necessary to explain why the average values of parameter ρ0 (Pm) for the sections in the first quarter are 10% higher than for the last, at the same values of phase angles ~ ±900. It can be assumed that, on average, the lunar regolith in the last quarter is represented by a more finely dispersed matter. It was here where late marine volcanism developed, and the surface soil can be enriched to date with microscopic ash particles smoothing the Pm polarization values. But perhaps, the answer must be sought in the difference between the mineralogical composition of the western and the eastern parts of the lunar disk. However, the identified correlation of these parameters makes it possible to calibrate the images synthesized as a function of the optical parameter of relative porosity ΔΨ of the lunar regolith in units of the H parameter proposed by Hapke.

Conclusion

In the given paper, data on the degree of maximum polarization are added to the Saari-Shorthill photometric catalog. The dependence of the second non-normalized Stokes parameter and the Hapke parameter is studied and a clear trend was identified that proves the relationship between them.

References

1.Kvaratskhelia O.I., Novikov V.V., Busarev V.V. Maturity factor of lunar regolith according to polarimetric observations // Proceedings of the Abastum Astrophysical Observatory. 1989. T. 68.pp.111-123.

2. Novikov V.V., Porosity of deposits of terrestrial and lunar basalts according to data on their albedo and degree of polarization // Complex research of the Moon. M.: Publishing house of Moscow State University, 1986, pp. 108-122.

3. Novikov V.V., Goryachev M.V. On the mechanism of interrelation of physical, mineralogical and optical properties of finely dispersed soils // Proceedings of GAI Sh. 1984. Vol. 56. pp. 113-125.

4.Dollfus A., Deschamps M. Grain size determination at the surface of Mars. Lunar and planet//Science.Houston,1985.V.16.pp. 193-199.

5.Hapke B., Optical properties of the lunar surface // Physics and astronomy of the Moon. Moscow: Nauka, 1973.pp. 166-229.

6.Saari J.M., Shorthill R.W. Photometric properties of selected lunar features .NASA. 1969.CR-29.187p.

7. Kvaratskhelia O.I, Spectropolarimetry of the lunar surface and lunar soil samples. Bull. Abastumani.astrophiz. observatory Gruz.An. 1988. No. 64. p. 312.

8. Kvaratskhelia O.I, Novikov V.V. Optical parameter of the relative porosity of the lunar regolith from polarimetric observations. Astron. Bulletin 1992. Vol.26. No. 6. pp. 3-13.

9. Kvaratskhelia O.I, International Scientific Konference ‘’Problems of Modern Astrofysics’’report “Spectropolarimetry of the Moon’’. Akhaltsikhe. 2015.

10. Kvaratskhelia O.I, Ivanidze R.,Gigolashvili Sh. Spectropolarimetry of the Lunar Surface and Ground Samples. Astronomy and Astrophysics(Caucasus)1, 2016, pp.49-52.

11. Kvaratskhelia O.I, Chigladze R., et.al. Multiparameter Atlas of the Moon. E.Kharadze Abastumani Astrophisical Odservatory.pp.1-180, 2019.

CATALOG KVARATSKHELIA-SAARI-SHORTHILL

N	λ^0	β^0	Hx100	ρ_0%	Pm% 440nm	ρ_0xPm	α^0	INDEX	Figure N
1	2	3	4	5	6	7	8	9	10
				First Quarter					
1	9,40	18,05	92,90	7,04	14,30	100,7	87,30	D16	4b
2	19,92	16,90	59,75	6,40	19,31	123,6	99,60	D17	4b
3	23,27	24,22	45,31	6,26	19,20	120,2	99,70	D18	4b
4	28,12	24,20	47,95	6,21	19,54	121,3	99,60	D19	4b
5	36,37	14,92	64,33	6,31	19,17	121,0	99,50	D20	4b
6	39,32	5,87	56,72	6,36	17,36	110,4	99,50	D21	4b
7	43,67	5,85	68,88	7,21	18,61	134,2	99,50	D22	4b
8	46,27	-0,05	51,97	6,68	16,53	110,4	99,50	D23	4b
9	51,33	-5,97	53,48	6,47	19,62	126,9	99,40	D24	4b
10	55,03	-4,23	59,46	6,94	12,60	87,4	99,40	D25	4b
11	59,35	-0,15	44,73	7,54	10,90	82,2	99,40	D26	4b
12	57,18	13,58	53,73	6,71	15,81	106,1	99,30	D27	4b
13	58,23	16,10	46,03	6,60	15,63	103,2	99,30	D28	4b
14	63,45	17,17	48,90	6,31	16,04	101,2	99,30	D29	4b
15	59,83	17,17	46,38	6,82	9,62	65,6	99,20	D30	4b
16	63,30	11,65	54,89	7,84	11,33	88,8	99,20	D31	4b
17	9,50	7,00			12,71		87,30	A16	5b
18	10,48	44,42	37,54	10,11	9,33	94,3	87,30	A15	5b
19	23,28	46,72	35,89	10,70	9,62	102,9	87,30	A17	5b
20	14,50	5,73	109,56	10,11	9,66	97,7	87,30	A18	5b
21	31,67	41,68	50,29	10,20	10,21	104,5	99,20	A19	5b
22	23,57	-1,82	104,33	9,98	9,33	93,1	99,00	A20	5b
23	37,15	-23,52	51,17	12,00	8,07	96,8	99,00	A21	5b
24	34,66	-3,38	65,94	10,69	9,64	103,0	99,00	A22	5b
25	38,42	-25,47	71,16	10,24	9,94	101,8	99,00	A23	5b
26	47,07	23,58	50,10	11,16	9,83	109,7	99,20	A24	5b
27	42,22	15,85	44,99	10,53	8,84	93,1	99,40	A25	5b
28	57,40	23,95	59,43	10,98	9,07	99,6	99,10	A26	5b
29	59,28	6,65	32,76	10,68	8,88	94,8	99,10	A27	5b
30	55,37	4,70	47,75	10,99	8,64	94,5	99,10	A28	5b
31	56,00	36,00	26,27	14,59	6,51	95,0	98,90	B31	6b
32	42,50	32,50	36,16	13,50	7,87	106,2	98,90	B32	6b
33	19,00	-6,00	62,54	13,98	6,61	94,5	98,80	B52	6b
34	21,00	-12,00	50,45	13,01	7,24	94,6	98,90	B54	6b

35	11,00	-28,00	51,04	13,31	8,26	109,9	87,30	B58	6b
36	68,00	-27,67	74,40	13,03	7,33	95,5	98,80	B63	6b
37	10,50	-27,50	53,52	14,10	7.92.	111,7	87,30	B68	6b
1	2	3	4	5	6	7	8	9	10
38	45,00	-42,00	84,13	14,29	6,65	95,0	98,80	B74	6b
39	30,00	-47,17	100,02	13,12	7,06	92,6	98,80	B76	6b
40	8,00	-53,00	52,36	14,17	7,00	99,2	87,30	B79	6b
41	11,50	-52,50	54,81	14,19	7,61	108,0	87,30	B80	6b
42	3,00	13,00	46,77	6,57	16,03	105,3	87,30	M15	7b
43	18,00	26,00	55,37	6,48	15,44	100,0	98,70	M16	7b
44	27,00	-4,50	105,19	7,23	14,24	102,9	98,50	M17	7b
45	26,00	44,50	60,38	8,88	10,66	94,7	98,70	M18	7b
46	30,00	7,00	75,85	6,42	17,07	109,6	98,60	M19	7b
47	30,00	54,00	65,19	7,38	9,28	68,5	98,70	M20	7b
48	35,00	-15,00	87,36	7,39	12,67	93,6	98,50	M21	7b
49	36,00	37,50	69,17	7,26	12,64	91,8	98,70	M22	7b
50	39,00	18,50	37,63	7,18	10,20	73,2	98,60	M23	7b
51	40,83	-46,75	50,90	15,18	6,13	93,0	98,50	M24	7b
52	52,75	-20,00	61,56	7,69	10,39	74,7	98,50	M25	7b
53	52,00	-2,50	63,12	6,55	15,28	100,1	98,50	M26	7b
54	59,00	17,00	47,67	7,74	15,24	102,7	98,60	M27	7b
55	7,03	-2,62	31,35	15,73	8,07	126,9	87,10	C6	8b
56	5,18	-7,42	89,90	19,68	6,48	126,5	87,10	C7	8b
57	12,50	6,25	11,13	12,32	9,61	118,5	87,20	C8	8b
58	15,10	3,98	11,09	10,11	11,45	115,8	87,20	C9	8b
59	15,40	-0,78	66,25	15,13	7,45	112,7	87,10	C10	8b
60	3,93	40,42	43,05	9,56	11,70	111,8	87,20	C36	8b
61	69,50	12,00	46,38	9,19	7,25	66,6	98,50	C50	8b
62	13,92	-13,73	31,78	12,02	8,06	96,9	87,10	C59	8b
63	44,08	-12,00	16,29	8,98	9,53	85,6	98,40	C60	8b
64	16,50	44,25	45,55	12,11	7,81	94,6	87,20	C69	8b
65	1,47	30,67	32,18	8,77	11,75	103,0	87,20	C75	8b
66	16,00	16,25	40,51	14,18	10,46	148,3	87,20	C76	8b
67	56,00	28,00	38,11	10,91	7,81	93,0	98,50	C79	8b
68	46,42	5,58	51,56	8,21	15,60	128,1	98,40	C88	8b
69	10,20	1,83	39,69	14,10	7,20	101,5	87,10	C112	8b
70	30,83	-10,83	40,71	10,89	8,20	89,3	98,30	R21	9b
71	0,08	38,60	30,66	8,13	11,06	89,9	87,10	R22	9b
72	54,50	-10,00	65,49	7,42	9,85	73,1	98,30	R23	9b
73	8,67	0,65	42,27	12,12	8,42	102,1	87,00	V2	10b
74	20,68	-4,92	47,84	14,87	7,00	104,1	87,00	V3	10b
75	14,22	-3,02	71,26	12,96	7,20	102,4	87,00	V4	10b

76	3,08	21,47	19,62	9,37	11,55	108,2	87,00	V6	10b
77	7,67	-0,98	45,51	12,64	7,54	95,3	87,00	V10	10b
78	6,50	-1,90	37,68	11,88	8,37	99,4	87,00	V11	10b
1	2	3	4	5	6	7	8	9	10
79	7,13	-10,80	58,20	11,97	8,06	96,5	87,00	V12	10b
80	39,52	-10,50	17,87	12,21	7,05	86,1	87,30	V13	10b
81	34,42	-1,28	34,49	10,21	8,42	85,9	87,30	V14	10b
82	6,25	26,07	88,29	7,62	11,51	87,7	87,00	V17	10b
83	20,32	-21,11	35,70	11,18	7,80	86,8	87,00	V18	10b
84	19,00	-16,58	41,00	13,31	7,51	99,9	87,00	V19	10b
85	19,67	-26,25	84,02	11,88	8,17	87,1	87,00	V20	10b
86	60,67	-25,17	75,95	13,73	8,29	113,0	87,70	T1	11b
87	57,08	-19,42	93,03	13,96	12,07	168,5	87,70	T2	11b
88	51,83	-31,83	31,67	20,30	8,67	174,8	87,70	T3	11b
89	47,62	-1,83	89,68	6,88	17,90	123,1	87,90	T4	11b
90	27,75	-28,00	46,61	12,97	7,91	102,6	87,70	T5	11b
91	32,72	-0,43	90,34	14,55	9,23	134,3	87,90	T6	11b
92	29,33	22,20	106,51	7,51	18,54	139,2	88,10	T7	11b
93	13,50	38,50	39,13	11,08	12,05	133,5	88,70	T11	11b
94	9,75	21,00	57,92	5,60	20,36	116,8	88,00	T12	11b
95	4,08	-4,75	54,54	11,19	8,91	110,9	87,90	T14	11b
96	17,33	20,70	56,11	7,08	19,20	135,9	88,00	T70	11b
97	39,53	36,08	47,53	7,93	9,75		89,00	T74	11b
98	22,00	13,50	59,05	5,75	21,51	123,7	88,00	T76	11b
99	6,80	13,00	47,20	6,22	18,22	113,3	88,00	T77	11b
100	16,12	41,37	47,27	11,32	9,63	109,0	88,70	T78	11b
101	38,50	44,07	6,08	11,50	10,81		88,70	T79	11b
102	20,42	-22,58	45,80	10,95	8,01	87,7	87,80	T83	11b
103	21,40	-22,58	55,97	11,53	8,51	98,1	87,80	T84	11b
104	22,08	-22,58	50,97	11,37	8,43	98,1	87,80	T85	11b
105	8,00	24,25	44,80	6,09	19,56	119,1	88,40	T86	11b
106	10,00	24,25	50,58	6,03	19,54	117,8	88,40	T87	11b
107	12,00	24,25	54,22	5,85	19,31	113,0	88,30	T88	11b
108	14,00	24,25	60,91	6,37	18,29	116,5	88,30	T89	11b
109	16,00	24,25	49,91	6,37	18,92	120,5	88,30	T90	11b
110	18,00	24,25	70,88	6,75	20,21	136,3	88,20	T91	11b
111	20,00	24,25	47,65	6,76	18,64	126,0	88,20	T92	11b
112	24,00	24,25	58,11	6,47	18,77	121,4	88,20	T94	11b
113	26,00	24,25	49,86	6,60	19,58	129,2	88,10	T95	11b
114	28,00	24,25	47,58	6,19	18,09	112,0	88,10	T96	11b
115	29,33	24,25	47,35	6,92	18,81	130,2	88,10	T97	11b
116	3,00	26,00	62,98	7,08	13,86	98,3	89,00	T98	11b
117	4,00	26,00	45,92	9,43	14,25	134,4	89,00	T99	11b
118	6,00	26,00	16,76	7,52	10,52	79,1	88,60	T101	11b
119	7,00	26,00	35,51	7,22	14,31	103,3	88,60	T102	11b

120	8,00	26,00	30,83	6,86	19,07	130,8	88,50	T103	11b
121	9,00	26,00	65,08	6,36	19,92	126,7	88,50	T104	11b

1	2	3	4	5	6	7	8	9	10
122	21,42	9,35	60,67	5,71	21,12	120,6	87,70	S1	12b
123	24,77	2,67	100,93	6,68	19,28	128,8	87,70	S2	12b
124	23,18	1,50	73,30	6,34	87,70	119,4	87,70	S3	12b
125	42,00	-0,85	18,55	7,07	87,40	91,1	87,40	P1	13b
126	35,45	0,10	61,32	9,41	87,40	120,5	87,40	P2	13b
127	26,08	0,57	61,13	6,48	87,50	123,7	87,50	P3	13b
128	13,23	0,05	57,21	11,57	8,57	99,2	87,60	P4	13b
129	36,92	4,17	20,09	6,80	18,93	128,7	87,40	P10	13b
130	34,00	2,75	61,97	6,62	17,18	113,73	87,40	P11	13b
131	24,17	6,75	55,57	6,71	19,51	130,9	87,50	P15	13b
132	35,25	2,92	51,35	6,61	17,42	115,2	87,40	P23	13b
133	20,25	3,33	83,20	6,25	16,74	104,5	87,60	P25	13b
134	24,52	0,45	64,68	6,67	18,06	120,5	87,50	P27	13b
135	21,50	0,33	101,94	6,69	15,28	102,2	87,50	P28	13b
136	13,50	-1,50	40,92	11,82	8,53	100,8	87,60	P36	13b
137	34,00	2,67	62,30	6,60	13,84	91,3	87,40	P47	13b
138	23,62	0,75	71,24	6,43	18,47	116,4	87,50	P48	13b

Last Quarter

1	-62,82	17,81	25,35	5,16	11,56	75,12	87,2	D1	4a
2	-79,95	24,68	42,39	6,5	12,00	78,00	87,3	D2	4a
3	-74,07	25,72	23,18	6,82	13,82	94,3	87,40	D3	4a
4	-68,90	24,45	31,63	5,70	15,71	89,55	87,40	D4	4a
5	-61,82	6,23	24,66	5,82	14,25	82,9	87,50	D5	4a
6	-67,20	-4,00	20,88	6,96	10,22	71,13	87,60	D6	4a
7	-56,85	-5,53	27,01	5,65	16,18	91,42	87,50	D7	4a
8	54,85	32,68	30,27	6,15	12,48	76,75	87,30	D8	4a
9	-46,73	19,77	29,66	6,82	14,03	95,68	87,30	D9	4a
10	-31,15	19,68	41,04	6,89	13,58	93,57	87,20	D11	4a
11	-21,05	24,42	48,27	6,73	13,27	89,31	87,20	D12	4a
12	-9,82	24,42	58,65	6,87	14,46	94,34	87,20	D13	4a
13	-5,65	12,00	59,50	6,68	13,46	89,9	87,30	D14	4a
14	11,32	-19,57	86,34	7,05	12,69	89,5	87,60	D16	4a
15	-73,53	-0,57	21,82	11,40	6,00	68,4	87,60	A1	5a
16	-62,10	-16,30	12,48	9,97	7,15	71,29	87,80	A2	5a
17	-51,28	-20,48	27,02	10,60	7,60	80,6	87,70	A3	5a
18	-50,40	-34,12	40,32	10,86	6,47	67,03	87,70	A4	5a
19	-26,17	11,53	27,62	10,84	8,27	89,7	87,80	A5	5a
20	-28,35	50,43	46,81	10,11	7,45	88,8	87,80	A6	5a
21	-6,40	-19,82	47,60	11,25	6,57	73,90	87,70	A10	5a

22	-4,63	-17,45	75,21	10,15	7,50	76,12	87,70	A12	5a
23	-4,60	-4,77	70,79	10,31	7,10	75,47	87,70	A13	5a
24	-64,35	-10,60	26,06	10,83	6,73	12,89	87,70	A29	5a
1	2	3	4	5	6	7	8	9	10
25	-74,53	-5,73	28,17	10,50	6,50	68,2	87,80	A30	5a
26	-28,00	67,50	41,52	14,24	6,10	86,9	87,90	B34	6a
27	-67,00	-22,00	20,63	14,09	6,64	93,6	88,10	B35	6a
28	-60,00	-23,50	34,97	14,48	6,23	90,3	88,10	B36	6a
29	-2,00	-29,00	49,77	13,65	5,83	79,6	87,90	B37	6a
30	-48,50	-31,00	43,31	1391,00	6,66	92,6	88,10	B38	6a
31	-12,00	-32,00	49,88	13,50	6,66	89,9	87,90	B39	6a
32	-19,17	-39,50	62,16	1375,00	6,45	88,7	87,90	B40	6a
33	-19,83	-40,67	32,26	14,15	6,30	89,1	88,00	B41	6a
34	-20,00	-42,50	49,71	14,12	6,40	90,4	88,00	B42	6a
35	-19,83	-45,00	40,74	1388,00	6,25	86,7	88,00	B43	6a
36	18,50	-45,17	73,73	15,00	6,05	90,7	88,00	B44	6a
37	-17,00	-49,00	58,46	14,02	6,25	87,6	88,00	B45	6a
38	-17,50	52,00	35,75	14,42	6,29	90,7	88,00	B46	6a
39	-7,50	-52,67	70,28	15,19	5,26	79,9	88,00	B47	6a
40	-2,50	-58,00	26,03	14,94	5,41	80,8	88,10	B48	6a
41	-29,00	-57,17	55,91	12,19	6,30	76,8	88,10	B49	6a
42	-37,50	-58,83	65,81	11,91	6,31	75,1	88,10	B50	6a
43	-20,50	-62,33	48,40	13,71	5,72	78,8	88,10	B51	6a
44	-65,00	-5,00	10,00	6,41	11,94	76,5	88,30	M2	7a
45	-54,00	-45,00	34,22	10,30	7,90	81,4	88,30	M3	7a
46	11,00	7,00	35,74	7,37	10,91	80,4	88,20	M4	7a
47	-45,50	54,50	75,62	8,11	9,02	73,1	88,30	M5	7a
48	-45,00	51,00	39,56	8,18	10,67	87,3	88,20	M6	7a
49	-39,00	-24,00	32,92	8,00	13,22	105,7	88,30	M7	7a
50	-32,00	45,00	38,25	6,74	13,05	84,4	88,20	M8	7a
51	-23,00	-11,00	49,44	6,24	15,87	99,0	88,30	M9	7a
52	-18,00	39,00	49,25	6,32	15,50	98,0	88,20	M10	7a
53	-15,00	-21,00	70,87	6,27	15,60	97,8	88,30	M12	7a
54	-8,00	12,00	60,80	7,06	12,75	90,0	88,20	M13	7a
55	-1,00	1,00	73,89	6,97	13,08	91,17	88,30	M14	7a
56	-44,20	-4,50	11,20	6,43	16,80	108,0	88,30	C1	8a
57	42,32	-7,80	28,30	6,50	16,41	107,6	88,50	C2	8a
58	29,55	-7,37	29,70	12,30	9,13	117,8	88,50	C4	8a
59	-9,50	51,50	38,29	6,55	13,21	86,5	88,40	C31	8a
60	-49,58	23,25	44,02	8,55	6,84	58,5	88,40	C39	8a
61	-4,00	29,67	81,56	7,40	11,89	88,0	88,40	C40	8a
62	-15,26	0,90	70,88	6,78	13,10	88,8	88,60	C44	8a
63	-14,00	-11,67	11,58	8,88	9,42	83,6	88,50	C53	8a

64	-66,83	-16,67	16,82	7,64	4,13	69,7	88,40	C62	8a
65	-23,83	-17,83	30,81	7,08	12,43	88,0	88,50	C64	8a
66	-67,33	2,00	24,40	11,17	8,32	92,9	88,40	C80	8a
1	2	3	4	5	6	7	8	9	10
67	-37,95	8,08	25,25	11,70	6,60	77,6	88,40	C81	8a
68	-20,00	9,67	24,19	14,09	7,21	101,6	88,40	C83	8a
69	-11,42	14,56	91,31	9,30	9,94	92,4	88,40	C84	8a
70	-2,08	-5,75	31,78	12,20	7,42	90,5	88,60	C91	8a
71	-39,83	-17,33	105,12	9,57	8,93	89,0	88,50	C94	8a
72	-22,25	-20,70	34,69	11,44	9,23	110,2	88,50	C95	8a
73	-32,45	-21,37	46,95	7,85	13,13	110,5	88,50	C99	8a
74	-11,30	-43,00	69,78	17,27	6,64	114,7	88,60	C102	8a
75	-4,00	-32,50	77,46	20,66	5,73	118,4	88,60	C104	8a
76	-26,73	2,00	19,08	7,29	12,18	88,8	88,70	R1	9a
77	-24,50	2,35	11,16	8,59	10,44	89,7	88,70	R2	9a
78	-26,80	9,33	15,89	9,05	11,46	103,7	88,70	R4	9a
79	-10,39	9,67	105,29	7,84	9,76	76,5	88,70	R5	9a
80	-20,33	-27,17	104,63	7,42	10,50	77,9	88,70	R6	9a
81	-19,63	-31,50	49,49	12,72	7,01	89,2	88,70	R7	9a
82	-19,25	-31,67	46,53	12,92	7,01	88,9	88,70	R9	9a
83	-4,00	-31,67	56,40	17,37	6,90	119,8	88,70	R10	9a
84	-45,00	22,85	25,28	7,35	12,60	92,6	88,80	R11	9a
85	-41,17	24,00	27,44	7,30	15,07	109,8	88,80	R12	9a
86	-42,17	20,42	25,37	7,21	14,46	104,2	88,80	R13	9a
87	-40,17	19,00	20,82	7,22	16,75	120,9	88,80	R14	9a
88	-38,00	16,00	19,73	7,47	14,32	107,0	88,80	R15	9a
89	-42,83	7,17	18,08	7,00	13,77	92,9	88,70	R16	9a
90	-39,75	9,25	13,58	8,15	12,10	98,6	88,70	R17	9a
91	-32,00	6,42	11,21	7,24	12,05	87,2	88,70	R18	9a
92	-39,17	12,00	21,62	7,31	12,40	90,6	88,70	R20	9a
93	-2,63	9,47	12,81	7,43	10,84	80,5	88,80	V1	10a
94	-4,17	16,48	72,00	7,41	9,80	77,5	88,80	V5	10a
95	-4,83	-4,67	40,60	10,34	8,34	86,2	88,80	V8	10a
96	-3,27	16,77	71,25	8,23	9,66	79,5	88,70	V15	10a
97	-4,47	20,92	67,79	6,54	14,90	97,4	88,80	V16	10a
98	-4,00	12,83	37,48	5,12	17,12	97,24	88,90	T18	11a
99	-2,67	49,50	46,24	10,73	10,56	113,4	89,00	T20	11a
100	-16,25	14,67	36,89	7,95	10,60	84,3	88,90	T24	11a
101	-20,30	10,42	28,26	12,39	7,21	89,3	88,90	T26	11a
102	-22,00	32,67	44,34	6,29	17,70	107,8	89,00	T27	11a
103	-30,92	13,17	57,28	7,34	12,50	91,7	88,90	T28	11a
104	-40,92	26,50	31,31	7,36	12,88	97,8	89,00	T36	11a
105	-45,95	12,60	18,83	6,83	17,30	118,2	88,90	T50	11a

106	-4,08	-13,67	98,15	9,19	8,60	74,0	88,90	T69	11a
107	-17,33	39,50	37,76	6,46	16,65	107,6	89,00	T71	11a
108	-38,67	42,00	48,51	8,97	9,40	84,3	89,00	T72	11a
1	2	3	4	5	6	7	8	9	10
109	-40,58	36,42	37,79	8,07	10,00	81,0	89,00	T73	11a
110	-39,53	36,08	47,53	7,98	9,75	75,8	89,00	T74	11a
111	-39,72	34,50	32,87	7,09	11,45	81,2	89,00	T75	11a
112	-19,30	38,50	44,07	6,08	17,91	108,9	89,00	T79	11a
113	-18,70	40,37	46,80	6,39	16,85	107,7	89,00	T80	11a
114	-59,00	10,00	30,81	5,77	17,55	101,3	88,90	T82	11a
115	-42,00	34,00	37,14	6,47	18,39	119,0	89,60	T105	11a
116	-47,50	12,50	33,94	6,14	18,35	112,7	88,90	T106	11a
117	-14,00	-22,00	78,35	6,39	19,45	124,0	88,90	T107	11a
118	-13,17	2,75	67,65	6,78	19,11	124,8	88,90	T108	11a
119	-20,58	-10,67	60,07	6,59	15,30	100,8	89,30	S2	12a
120	-2,33	-12,92	47,77	10,04	8,66	86,9	89,30	S4	12a
121	-43,33	-2,33	35,00	5,33	19,60	104,5	89,30	S5	12a
122	-23,17	-3,33	34,83	6,36	15,00	95,4	89,30	S6	12a
123	-1,48	0,47	89,85	6,90	13,88	95,8	89,30	S8	12a
124	-11,43	-41,02	95,08	13,82	6,90	95,4	89,30	S9	12a
125	-64,55	7,00	21,87	6,70	15,60	104,5	89,30	S10	12a
126	-62,05	18,87	27,03	5,45	12,44	95,0	89,30	S11	12a
127	-19,57	-11,32	53,50	6,38	14,71	93,8	89,30	S13	12a
128	-1,45	0,02	88,32	6,92	19,20	133,0	89,10	P5	13a
129	-1,93	-3,93	110,00	10,50	11,10	116,5	89,10	P6	13a
130	-22,10	-3,52	27,26	6,74	15,80	105,1	89,20	P7	13a
131	-36,57	-2,98	33,13	5,75				P8	13a
132	-43,48	-1,97	24,35	5,55	19,20	106,6	89,20	P9	13a
133	-13,00	1,00	63,67	6,85	14,45	90,7	89,10	P18	13a
134	-27,17	3,47	24,33	7,23	10,88	78,7	89,10	P19	13a
135	-42,33	1,50	32,35	5,54	18,80	104,1	89,20	P22	13a
136	-27,45	0,62	22,15	7,35	18,75	137,8	87,50	P26	13a
137	-23,25	-3,08	43,16	6,52	15,32	99,9	89,20	P31	13a
138	-37,17	-3,17	32,80	5,66	18,92	107,1	89,20	P33	13a
139	-43,80	-2,47	30,11	5,25	19,01	104,0	89,20	P34	13a
140	-1,33	0,92	63,40	6,85	12,31	84,3	89,10	P37	13a
141	-9,00	5,00	63,32	5,50	18,52	101,9	89,10	P38	13a
142	-20,00	-0,50	37,61	7,00	13,53	94,7	89,10	P41	13a
143	-22,08	1,17	16,03	9,41	9,95	93,6	89,10	P42	13a
144	-23,25	-3,03	43,16	6,52	15,32	99,9	89,20	P43	13a
145	-43,92	-2,33	27,67	5,26	17,81	93,0	89,20	P46	13a
146	-1,33	0,42	87,22	6,94	10,16	70,5	89,10	P49	13a

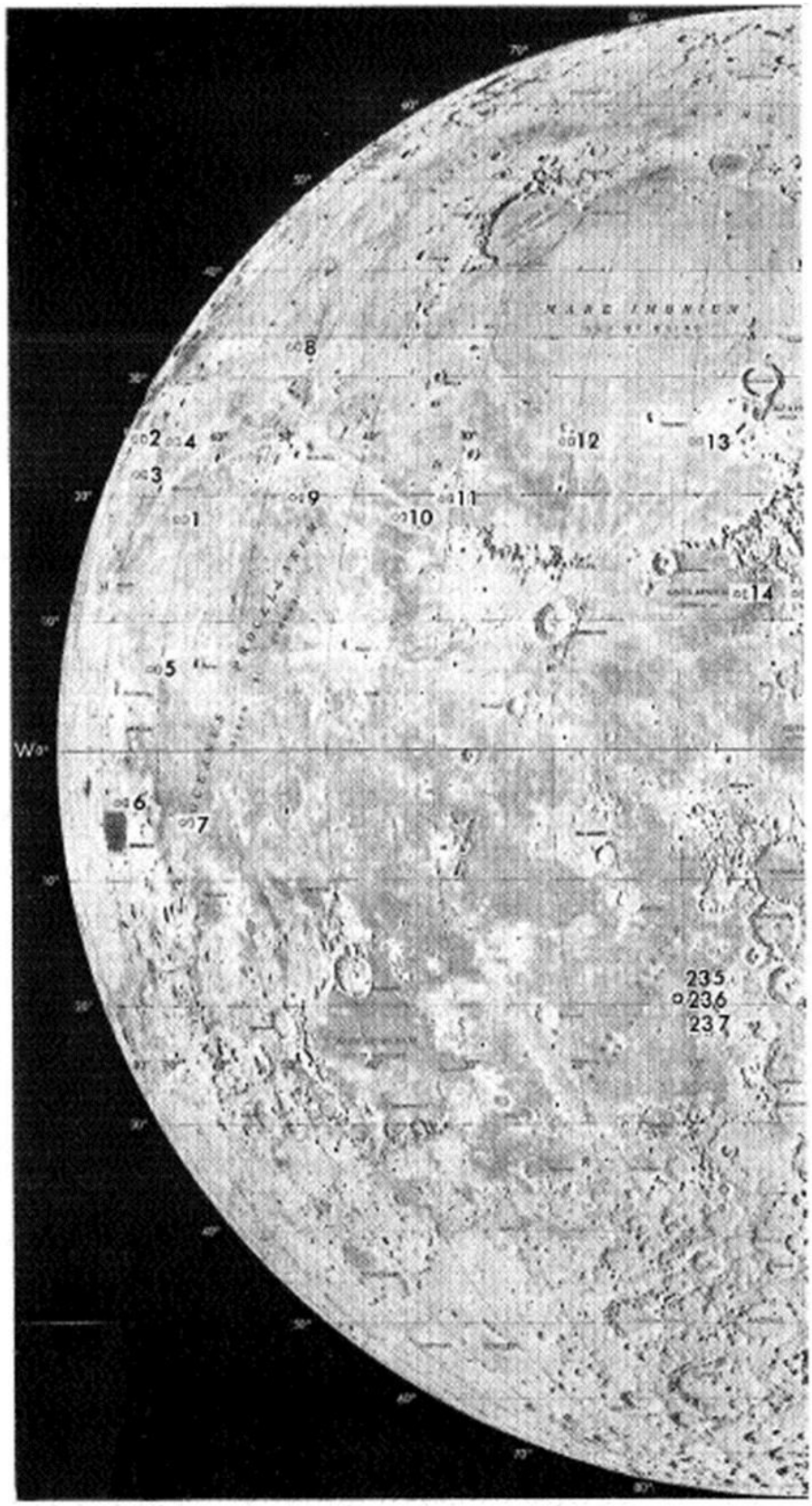

Figure 4a. Locations of dark albedo sites on the lunar disk.

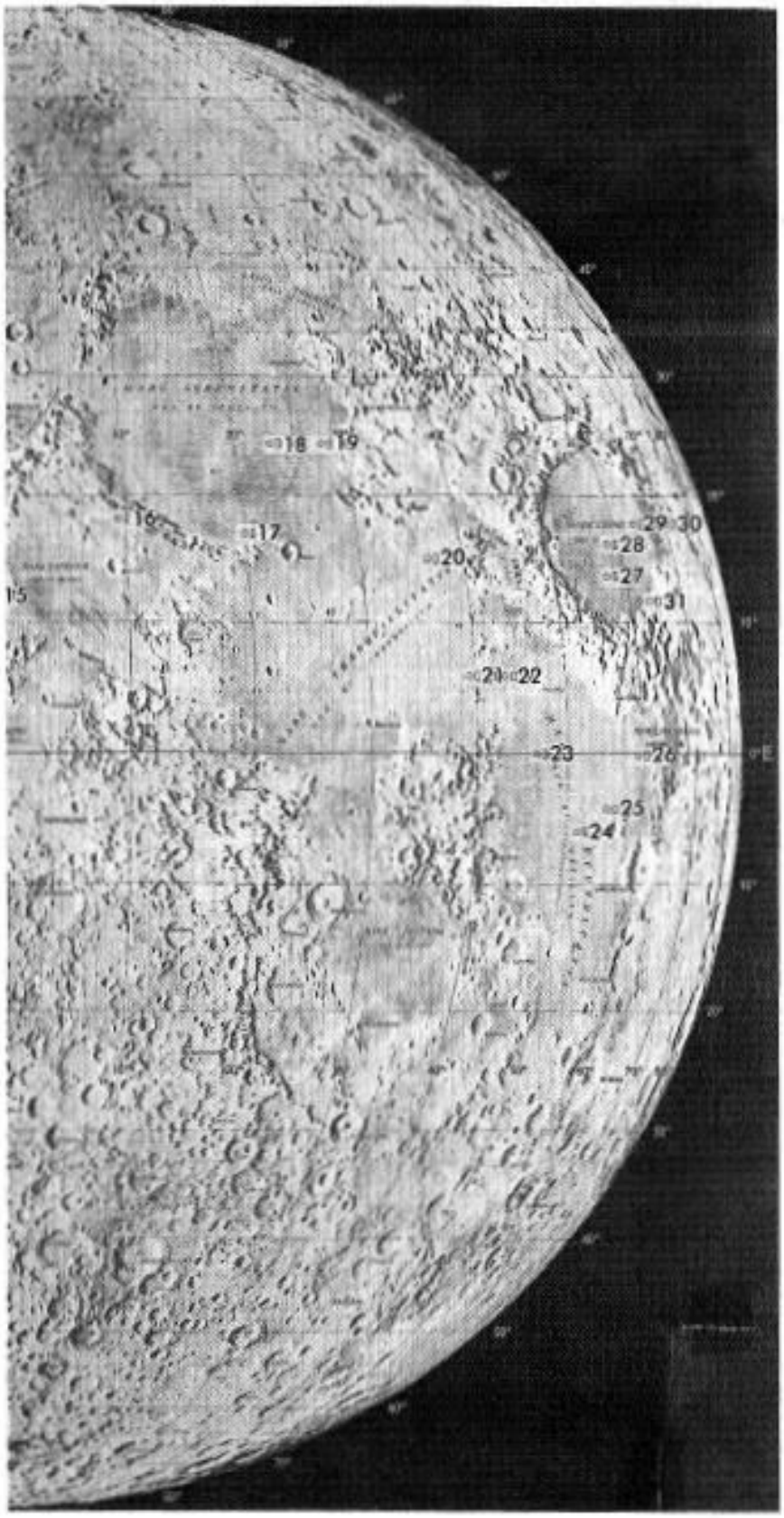

Figure 4b. Locations of dark albedo sites on the lunar disk.

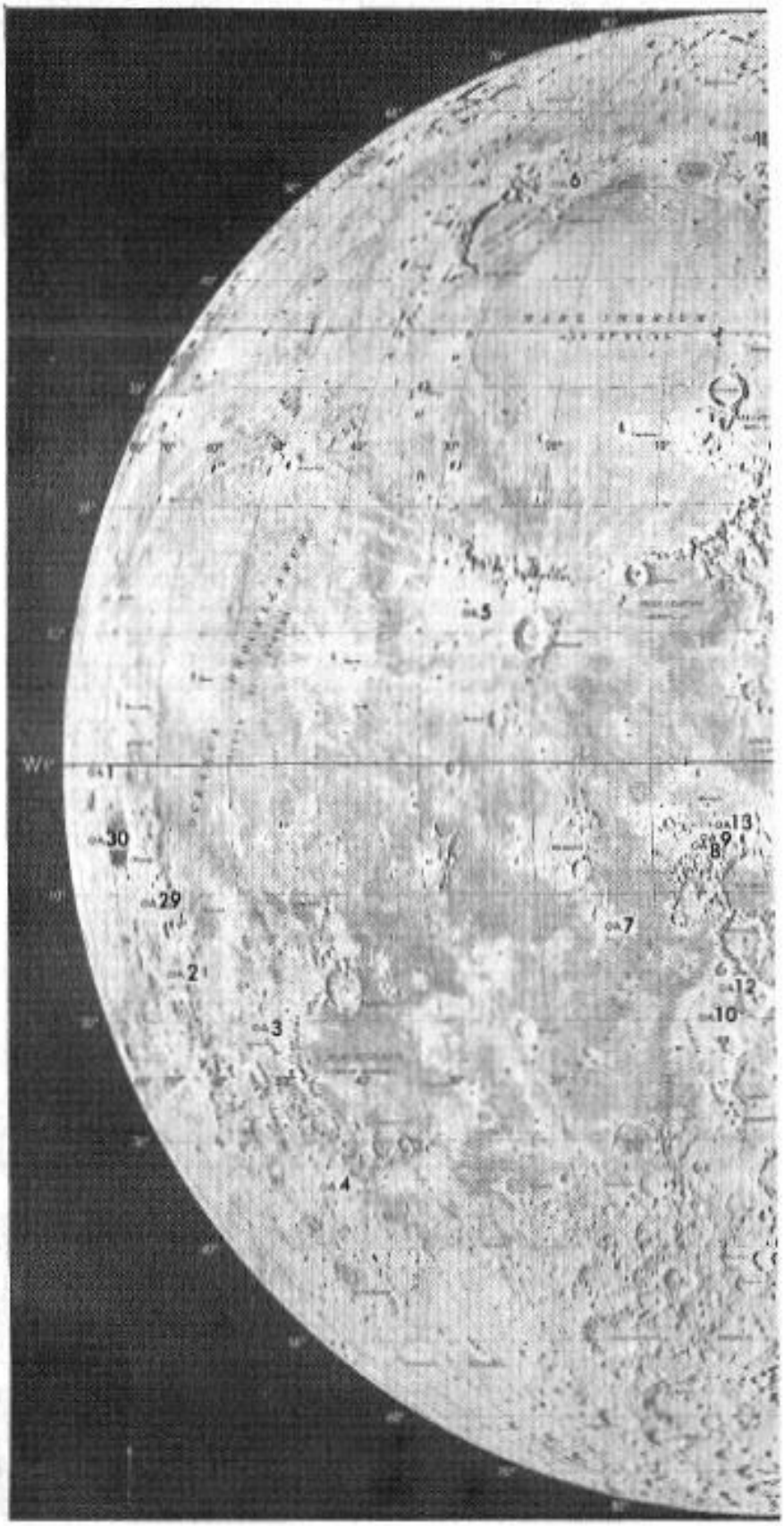

Figure 5a. Locations of average albedo sites on the lunar disk.

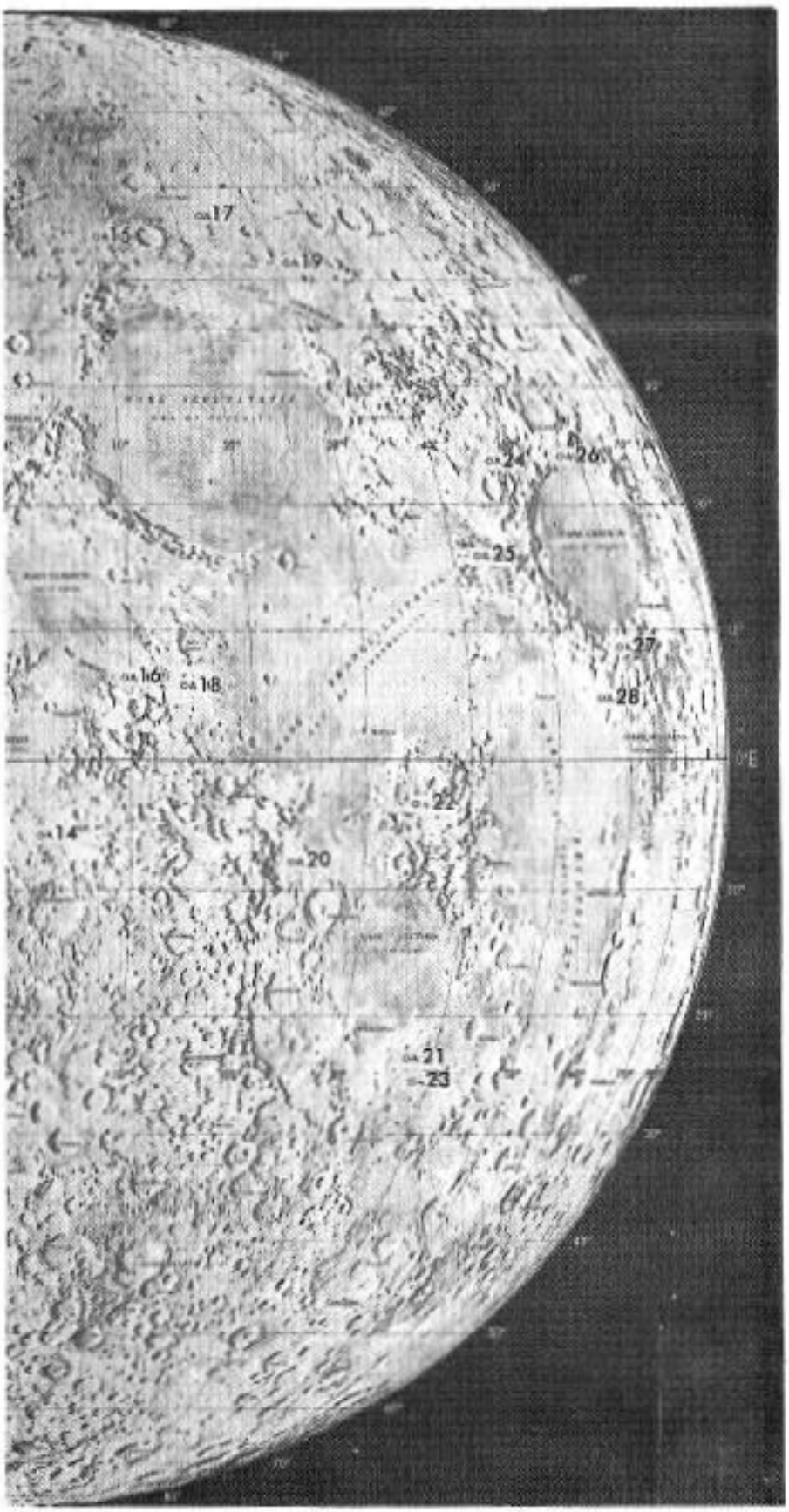

Figure 5b. Locations of average albedo sites on the lunar disk.

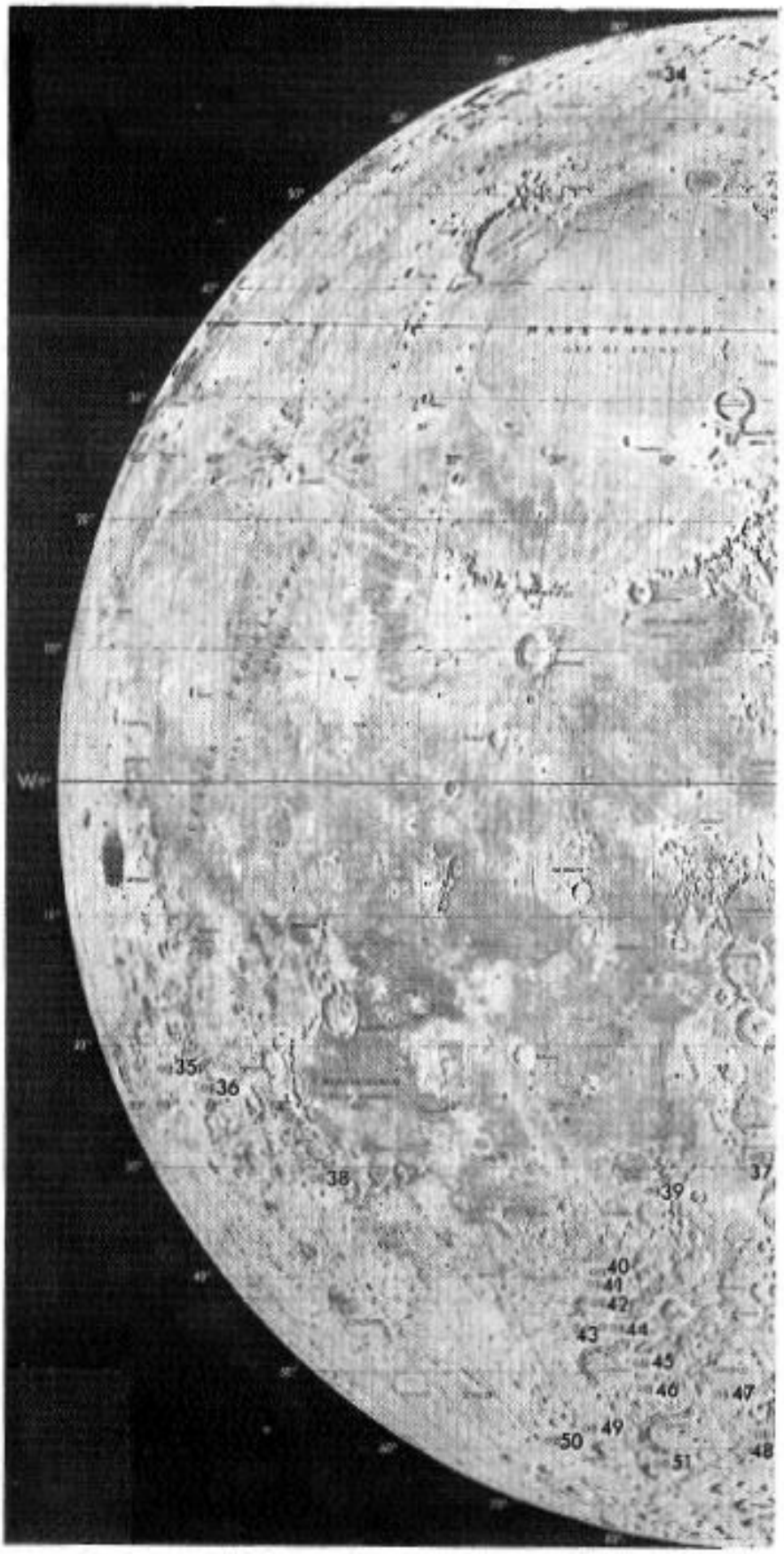

Figure 6a. Locations of bright albedo sites on the lunar disk.

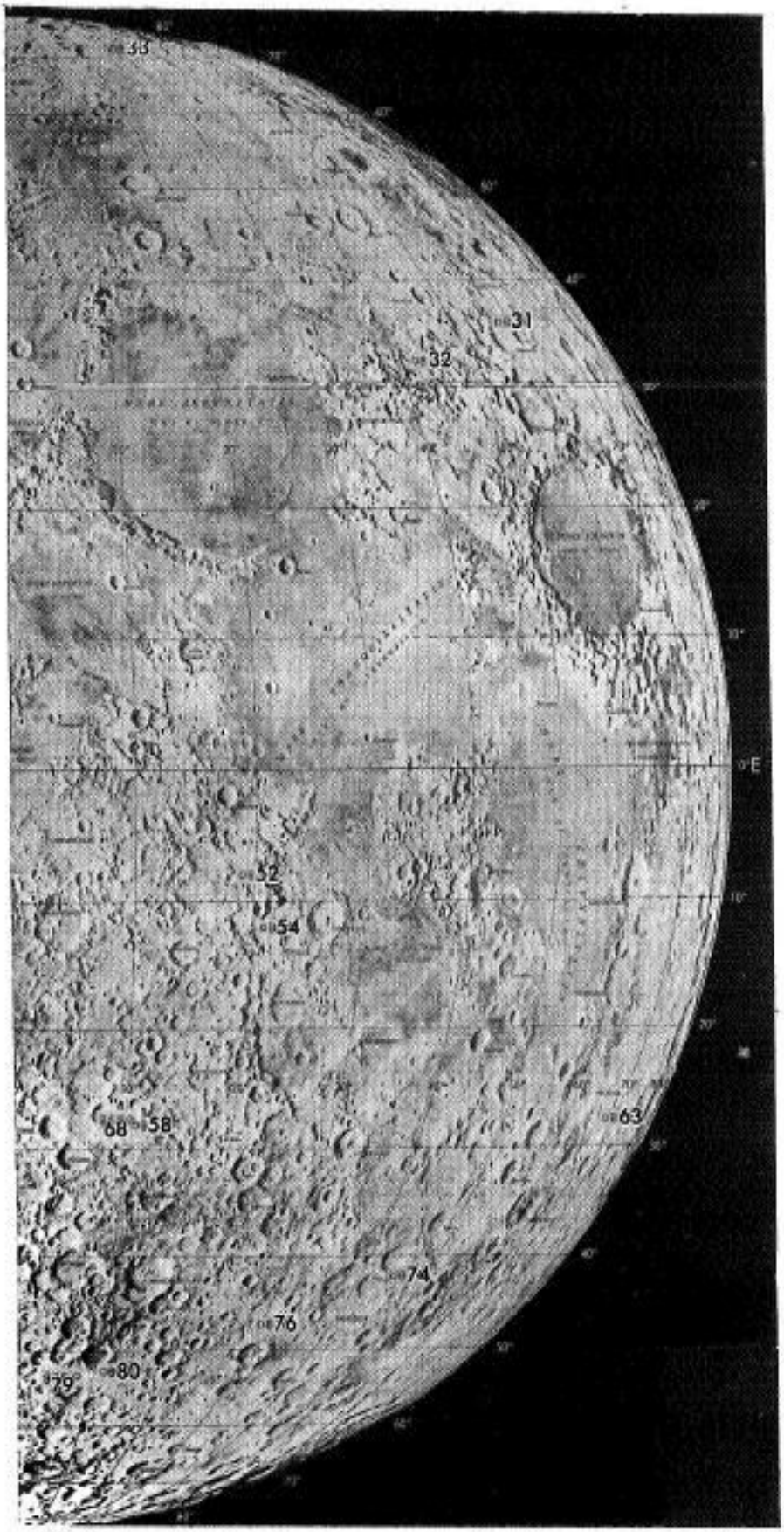

Figure 6b. Locations of bright albedo sites on the lunar disk.

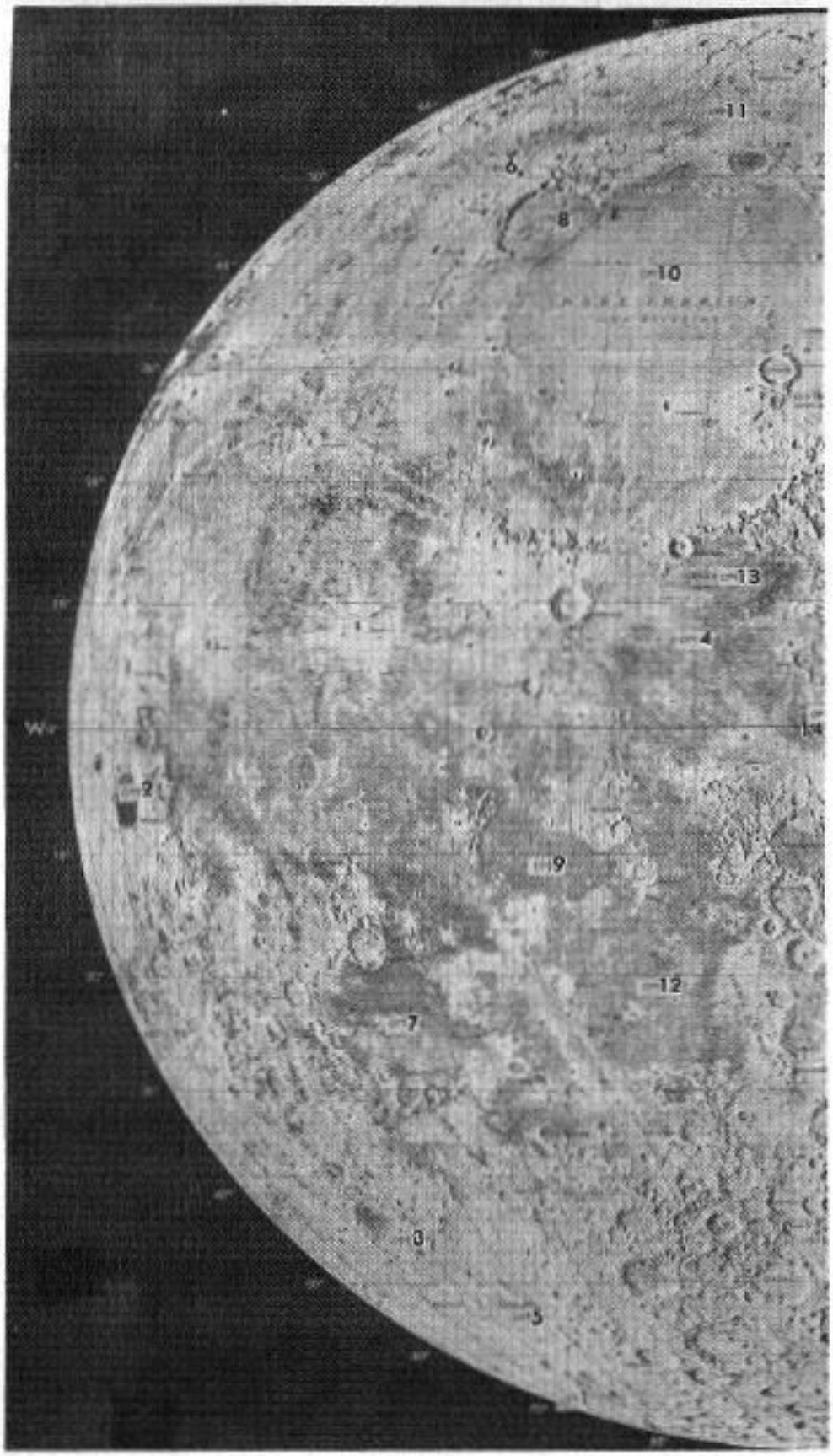

Figure 7a. Locations of mare sites on the lunar disk.

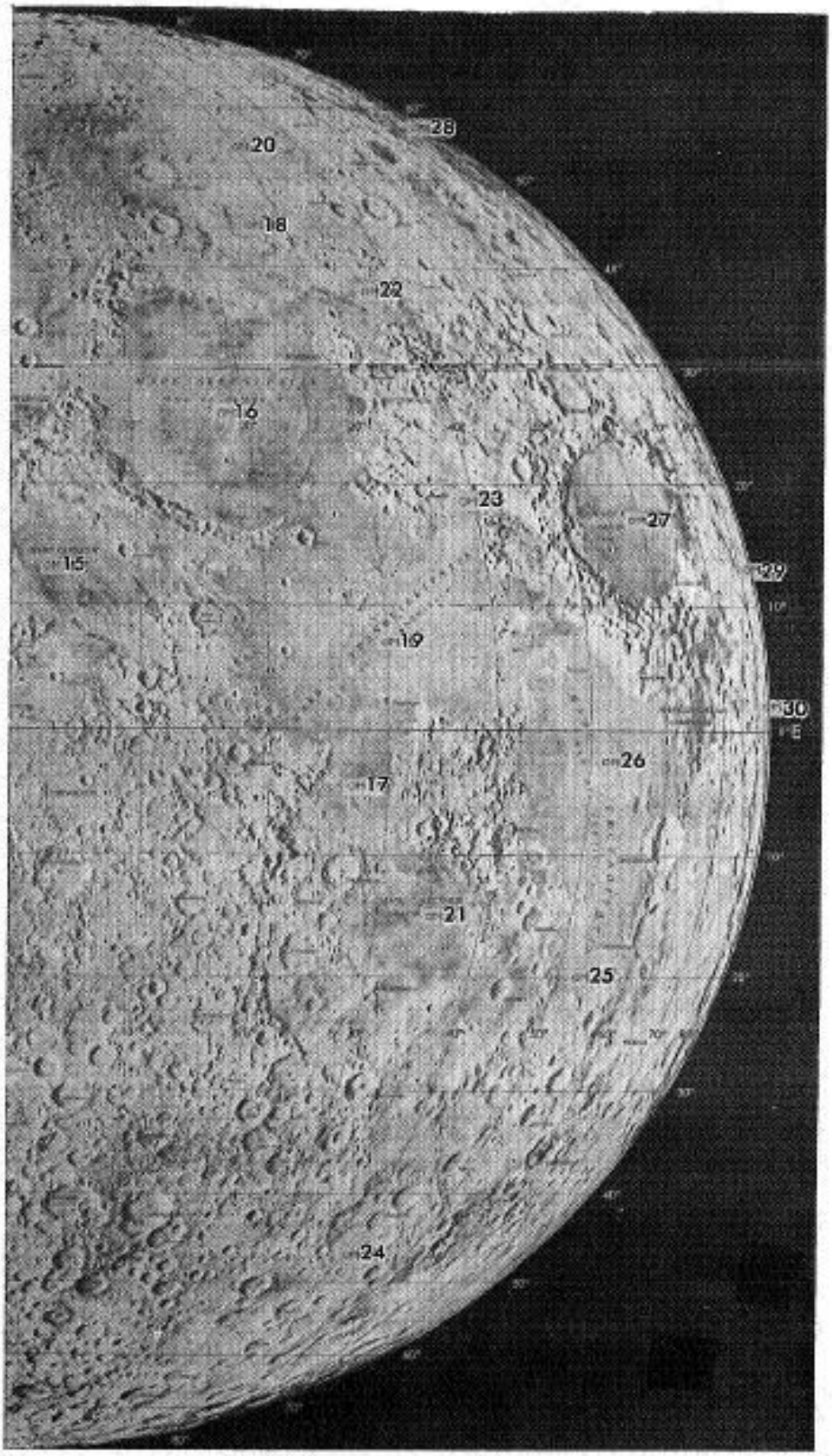

Figure 7b. Locations of mare sites on the lunar disk.

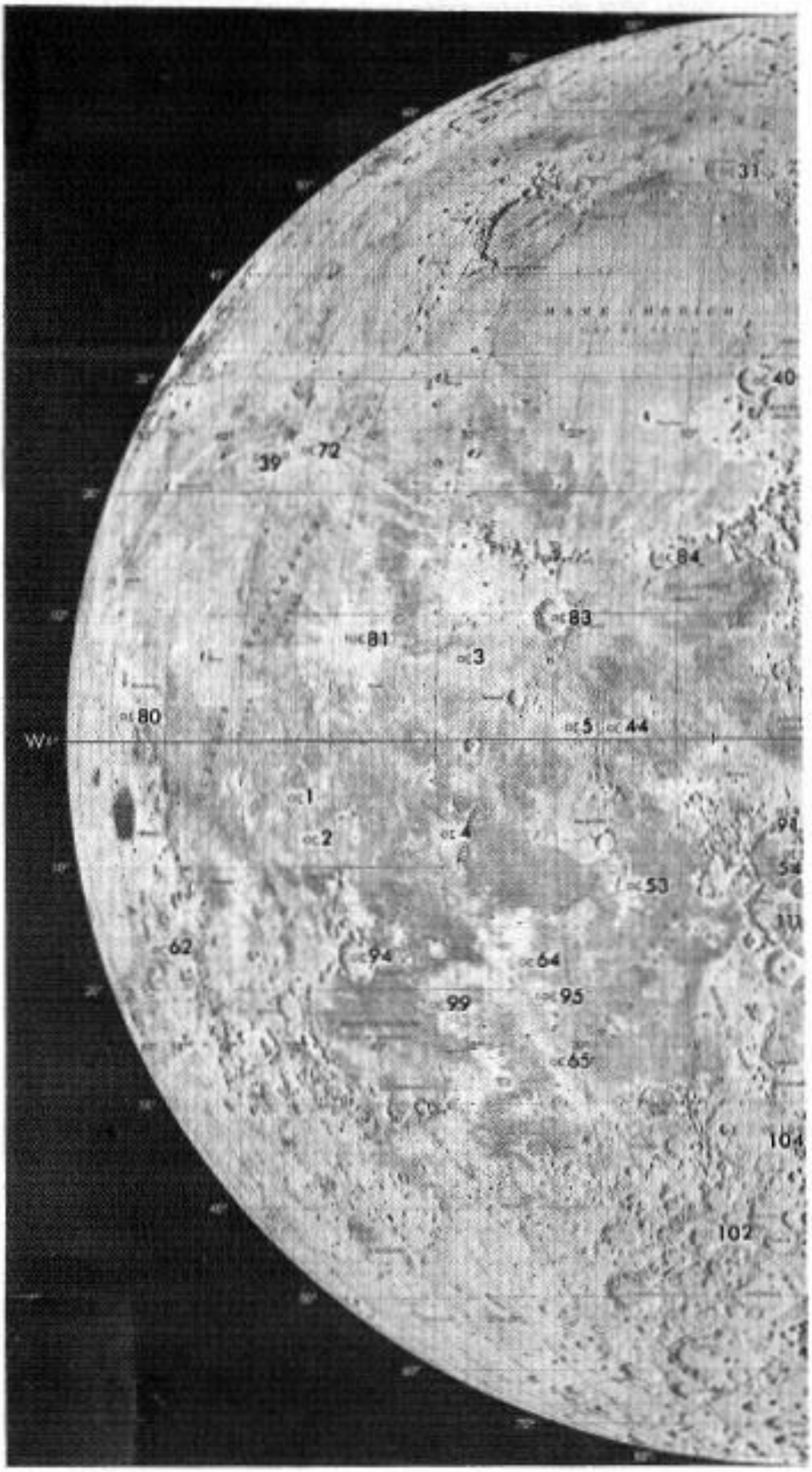

Figure 8a. Locations of crater sites on the lunar disk.

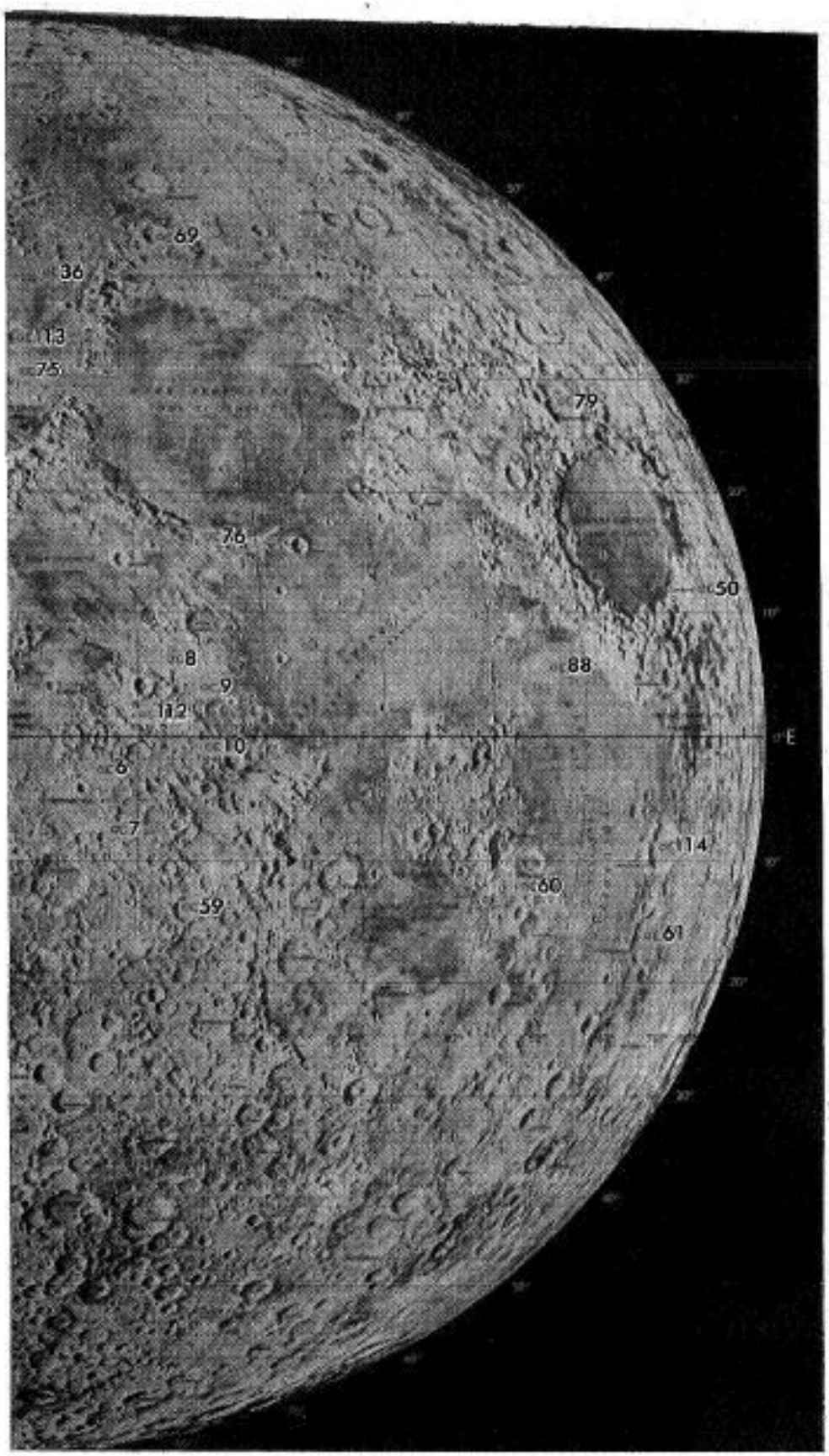

Figure 8b. Locations of crater sites on the lunar disk.

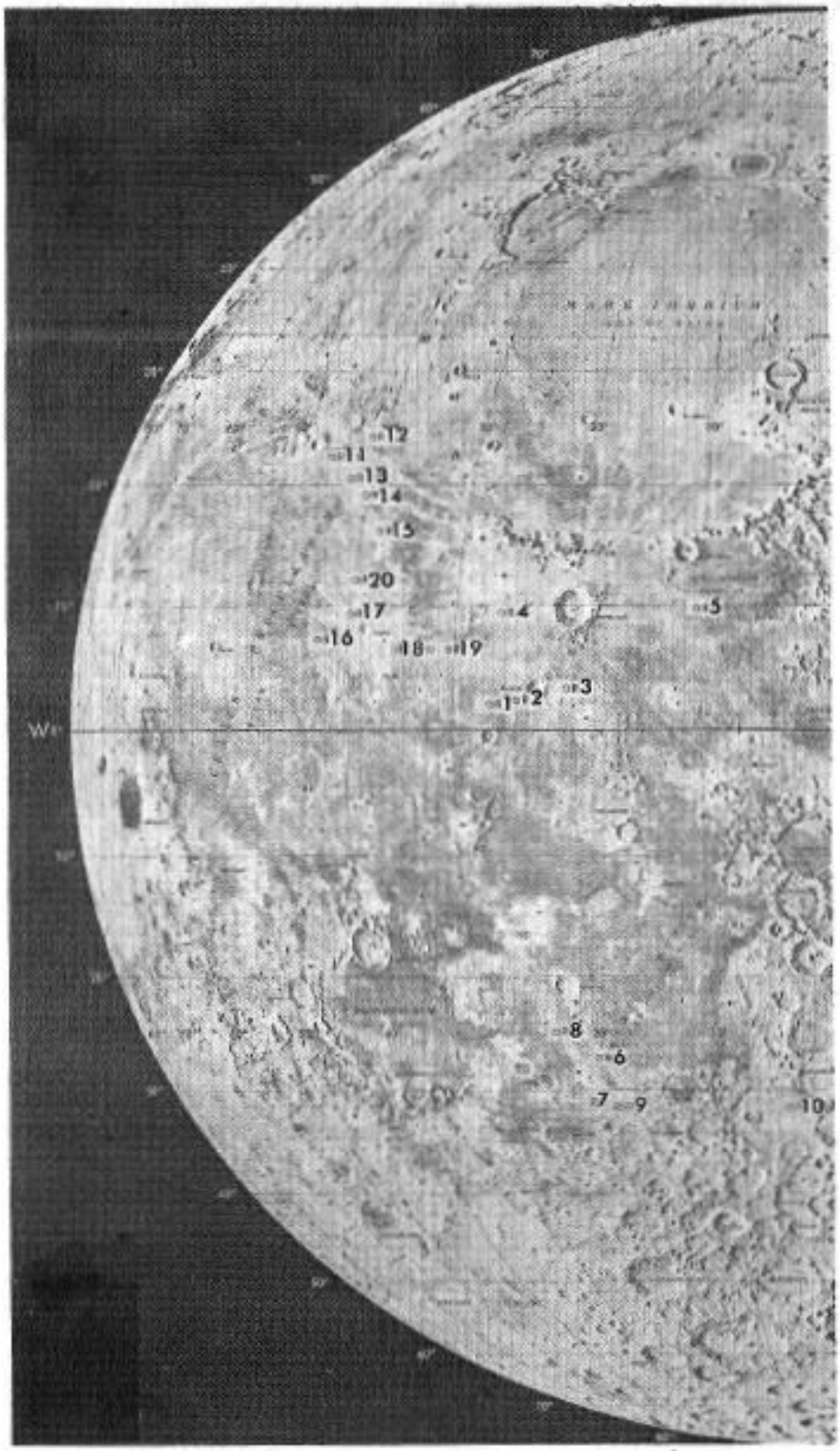

Figure 9a. Locations of ray sites on the lunar disk.

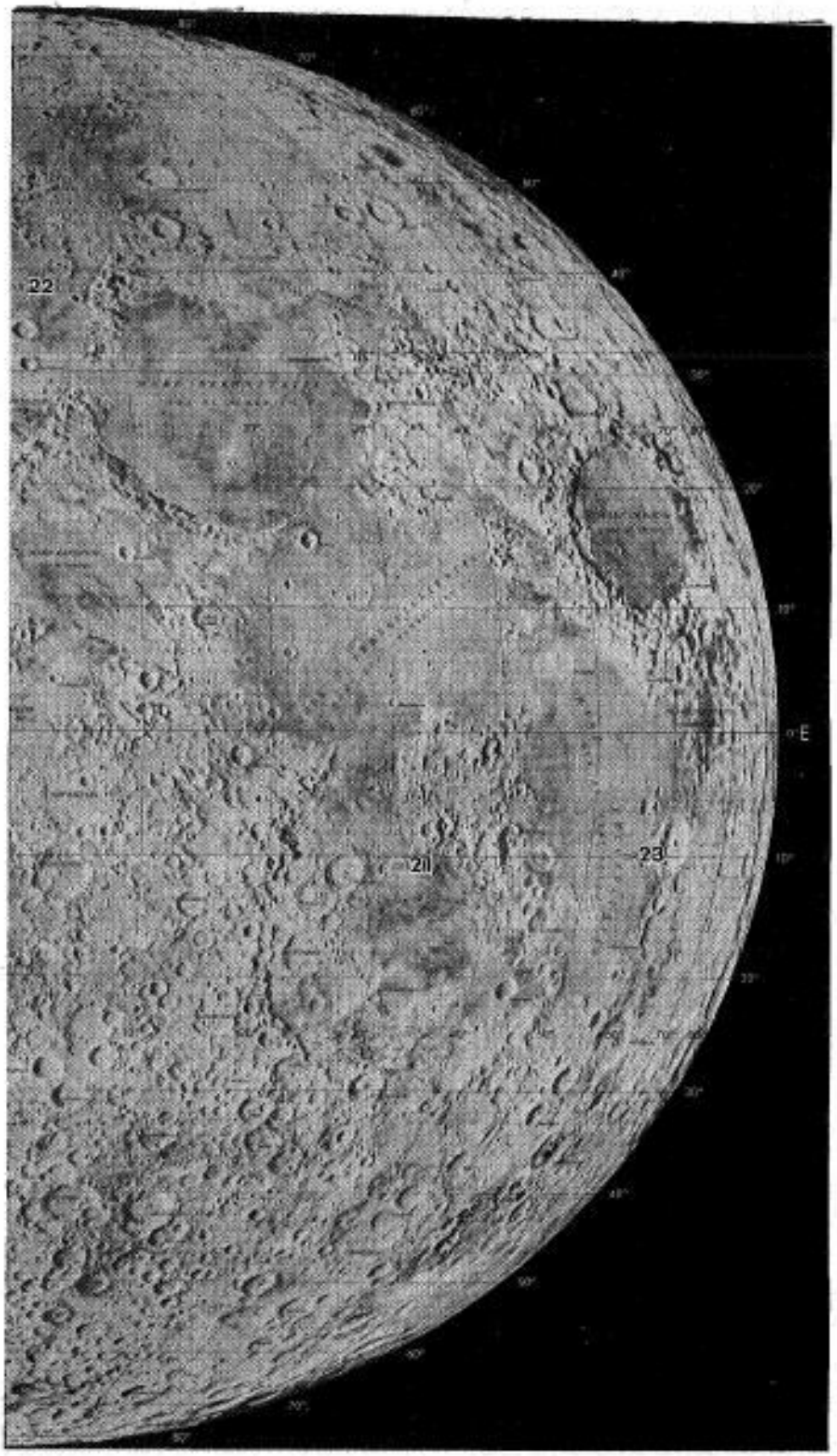

Figure 9b. Locations of ray sites on the lunar disk.

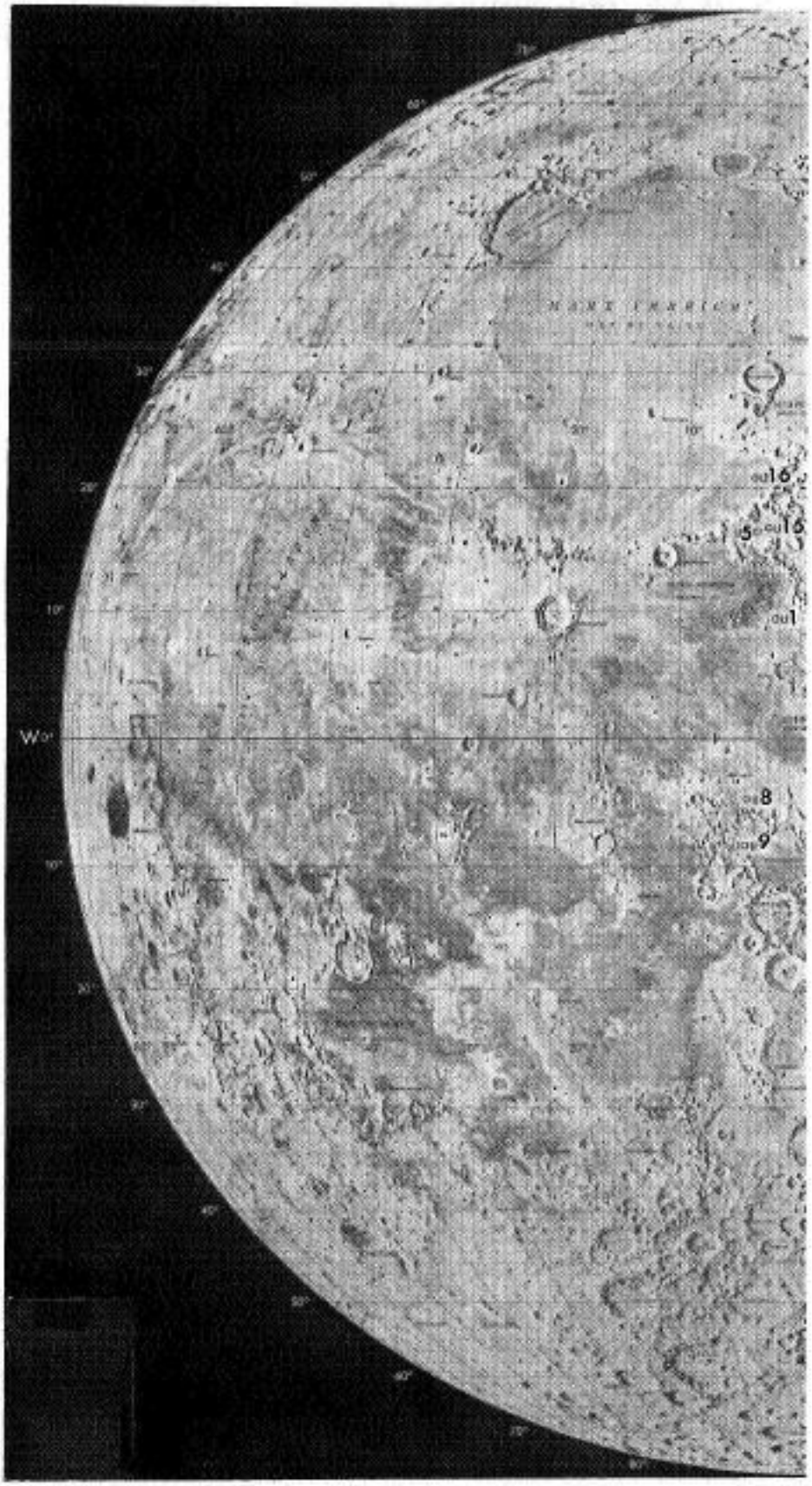

Figure 10a. Locations of upland sites on the lunar disk.

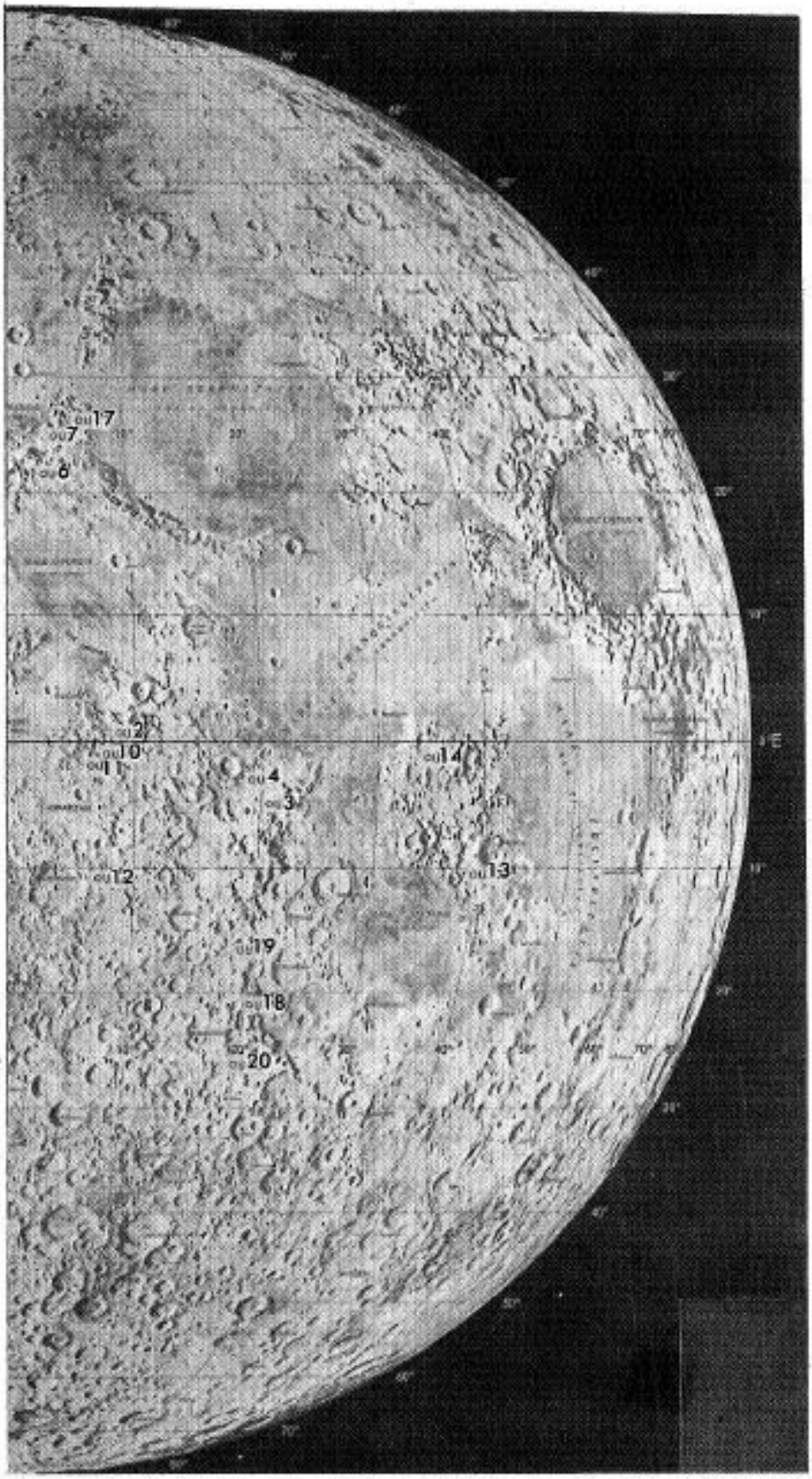

Figure 10b. Locations of upland sites on the lunar disk.

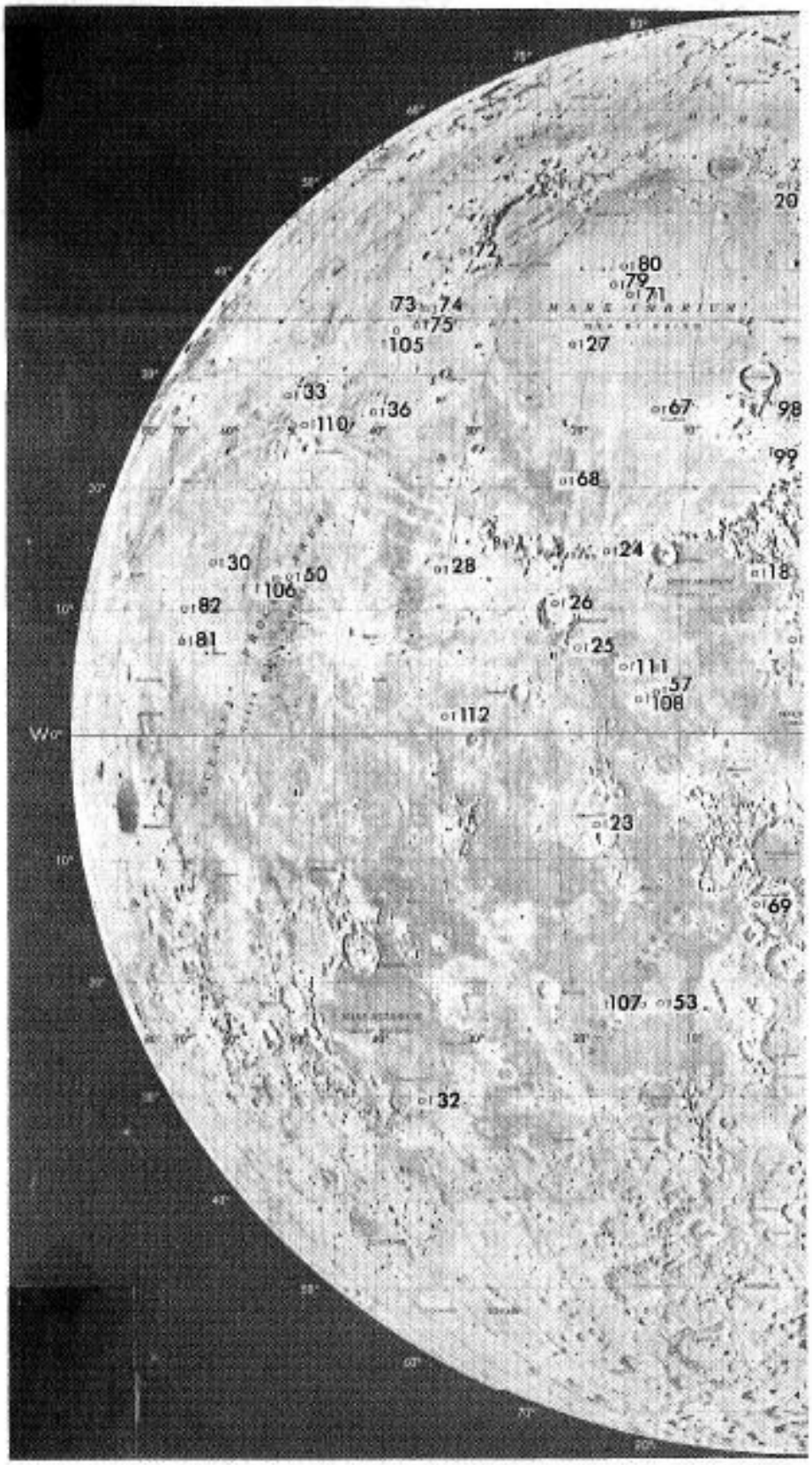

Figure 11a. Locations of scientific sites on the lunar disk.

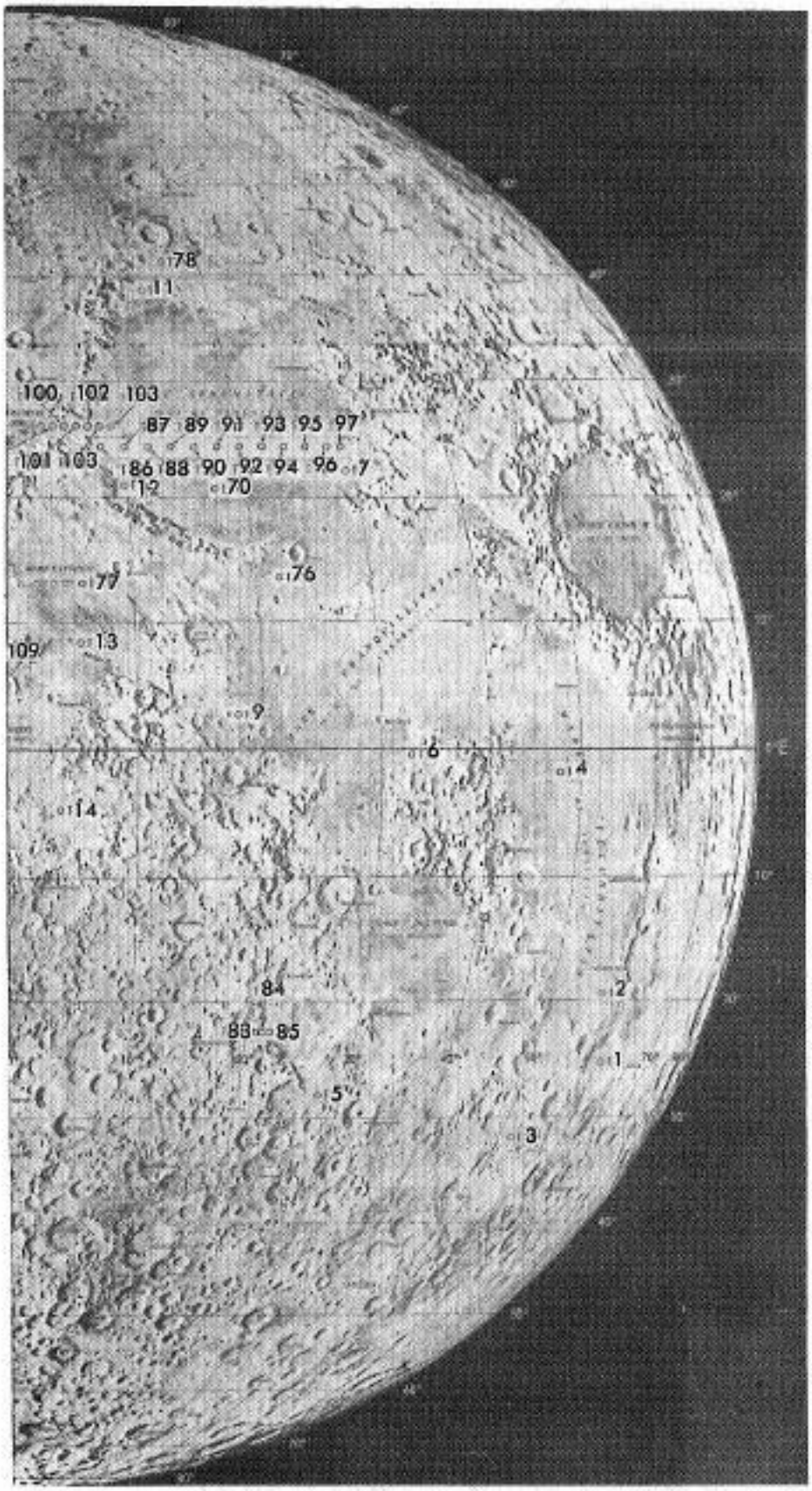

Figure 11b. Locations of scientific sites on the lunar disk.

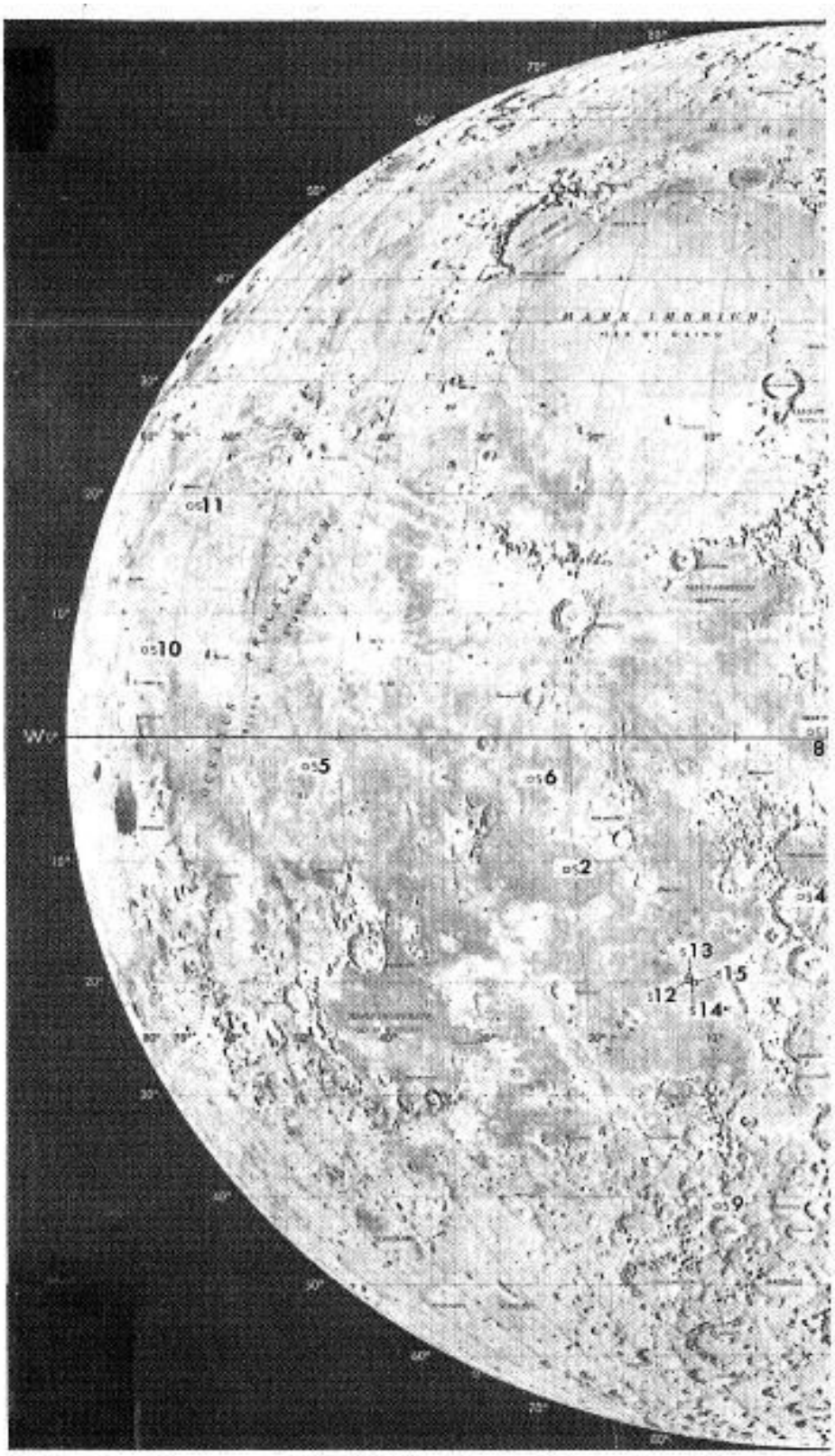

Figure 12a. Locations of spacecraft sites on the lunar disk.

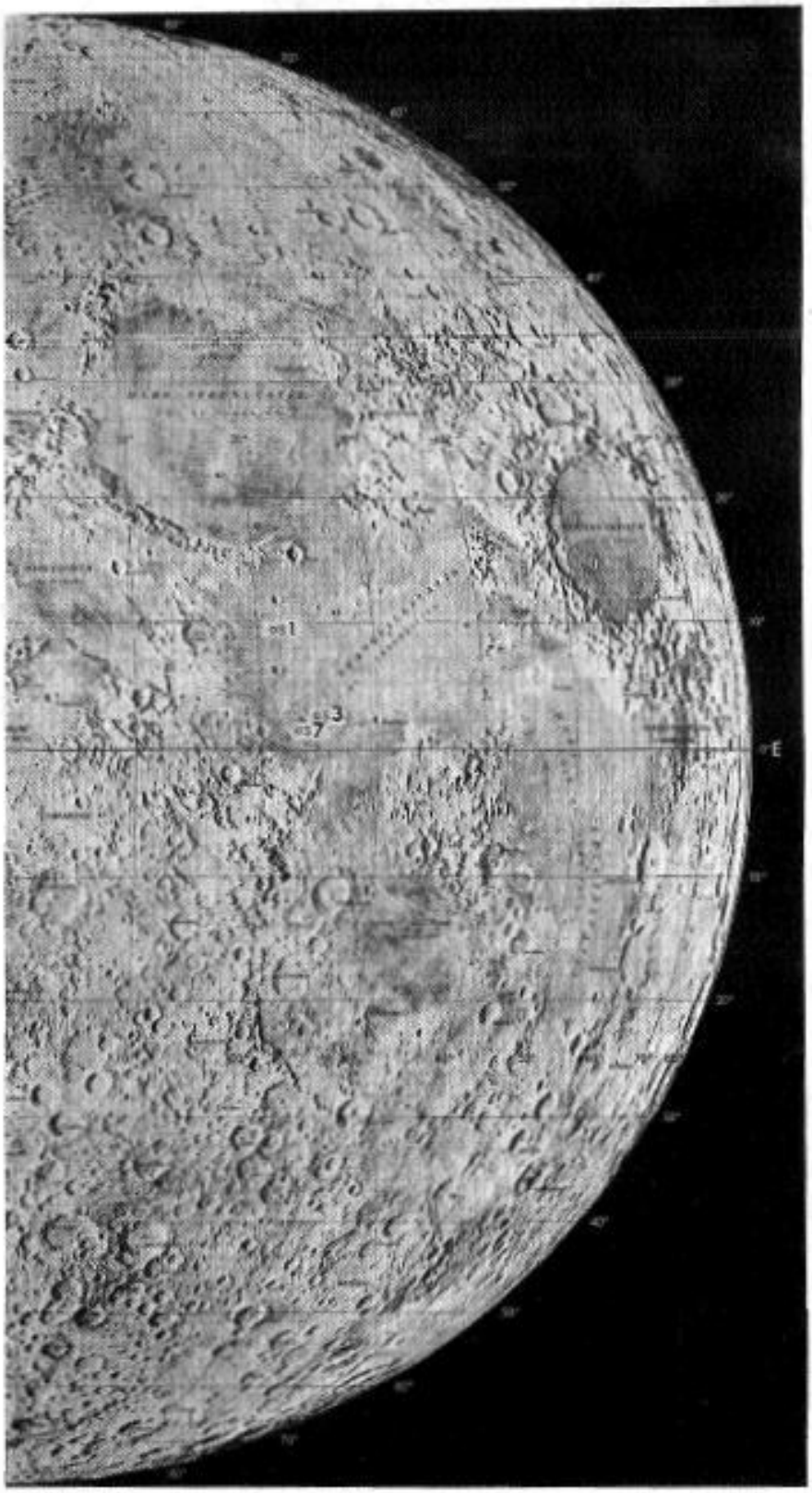

Figure 12b. Locations of spacecraft sites on the lunar disk.

Figure 13a. Locations of Apollo sites on the lunar disk.

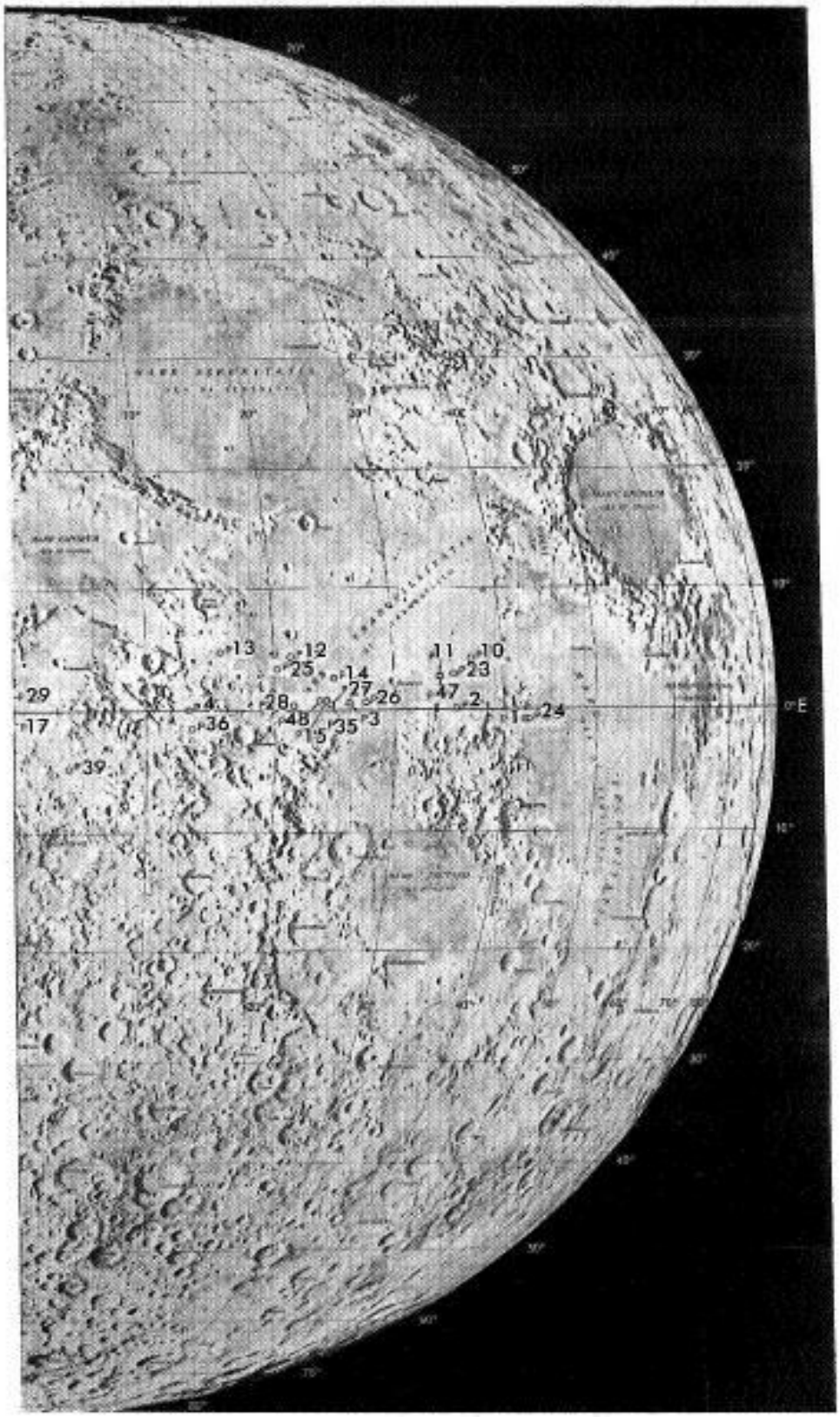

Figure 13b. Locations of Apollo sites on the lunar disk.